

# Hydrothermal Fluid Evolution at the Batu Hijau Cu-Au porphyry Deposit, Indonesia

Schirra M.<sup>1</sup>, Zwyer T.<sup>1</sup>, Driesner T.<sup>1</sup>, Heinrich C.A.<sup>1</sup>

1) Eidgenössische Technische Hochschule, Zürich, Switzerland

## Introduction

The giant Cu-Au porphyry deposit Batu Hijau is located in the southwestern part of Sumbawa Island, Indonesia. It is associated with multiple generations of low-K tonalite porphyry intrusions emplaced at shallow depths ( $\leq 2$  km) into volcano-sedimentary sequences around 3.7 Ma ago (Meldrum et al., 1994; Garwin, 2000). Volatile components expelled from the intrusions during emplacement and subsequent crystallization initiated a hydrothermal system fed by fluids from an inferred larger magma chamber below, which produced intense alteration and stockwork vein formation. Based on cross cutting relationships a time sequence of vein formation, correlating with the evolution of the hydrothermal fluid, can be established (Gustafson & Hunt, 1975). Copper-iron sulfides typically occur within different generations of quartz veins formed during early alteration or less frequently as later sulfide veinlets associated with transitional alteration (Mitchell et al., 1998; Clode et al., 1999). Principal ore minerals are chalcopyrite and bornite together with minute blebs of native gold (Arif & Baker, 2004). Fluid inclusions (FIs) entrapped within different vein generations record the chemical and physical evolution of the hydrothermal fluid and can provide information about sulfide precipitation conditions. Based on FIs, Garwin (2000) described vein formation temperatures decreasing from 700°C to <400°C. However, later studies focused on FIs reported constant temperatures around 300°C and pressures around 50 bar, supposedly independent of vein types and contained sulfides (Imai & Ohno, 2005; Imai & Nagai, 2009).

During the last decade, cathodoluminescence (CL) imaging has become increasingly popular in FI studies focused on porphyry copper deposits (e.g. Rusk & Reed, 2002, 2006; Landtwing et al., 2010; Rottier et al., 2016). In several cases quartz textures obtained by CL-imaging showed that ore minerals were introduced by reopening of previously formed quartz veins (e.g. Redmond et al., 2004; Landtwing et al., 2010; Frelinger et al., 2015). Since quartz veins host most of the FIs, the timing of quartz relative to sulfide precipitation is essential for determining accurate temperature and pressure conditions of ore formation.

The aim of the present work is to refine the present model of ore formation at the Batu Hijau porphyry Cu-Au deposits regarding its fluid history. FIs entrapped in different vein types will be investigated using conventional petrography, CL imaging and microthermometry in order to constrain the physical conditions of vein formation as well as ore precipitation, extending the work of Zwyer (2010).

## Mineralization, Alteration and Veining

Mineralization at Batu Hijau is related to the emplacement of multiple porphyry tonalite stocks (Meldrum et al., 1994; Mitchell et al., 1998; Garwin, 2000). Three generations can be distinguished: 1) old tonalite (OT), 2) intermediate tonalite (IT), and 3) young tonalite (YT; Mitchell et al., 1998; Proffett, 1998). The small-volume OT and dominant IT are intensely mineralized but difficult to distinguish, while the YT intrusion is only weakly mineralised. The shell-shaped ore body is situated at depths between 150 and 900 m below the pre-mining surface. Highest ore grades with ppm Au/wt.% Cu ratio >1 by weight are in the upper central part of the ore shell, while the deeper periphery is generally of lower grade with Au/Cu ratio <1. At greater depths, a sharp drop in ore grades in combination with high vein densities delineates the barren core.

Excluding the barren core, ore grades at Batu Hijau correlate with vein density (Mitchell et al., 1998), which indicates their importance for mineralization. Based on geometry, mineralogy, associated alteration, and mutual time relationships veins can be classified into five different types: A-, AB-, B-, C-, and D-veins in chronological order (Mitchell et al., 1998; Clode et al., 1999; Imai & Ohno, 2005; Zwyer, 2010).

*A-type veinlets* represent the earliest hydrothermal products. They are typically thin, discontinuous, quartz-dominated veins with irregular wall contacts (Fig. 1A). Besides quartz, magnetite is a common mineral that occurs in the early formed veins (Am-veinlets, Fig. 1B).

*AB-veins* are the most abundant vein type in Batu Hijau. They represent a transition from earlier A-veinlets to later B-veins as evidenced by cross cutting relationships. In contrast to A-type veinlets, they are thicker (up to 8 cm), show more regular wall contacts, and straighter propagation. However, compared with later B-veins, they are still undulated. In the mineralized region, bornite and chalcopyrite appear as either disseminated grains or massive accumulations within the quartz veins (Fig. 1B). In the deeper parts, AB-veins are barren and occasionally contain magnetite, often along wall rock contacts.

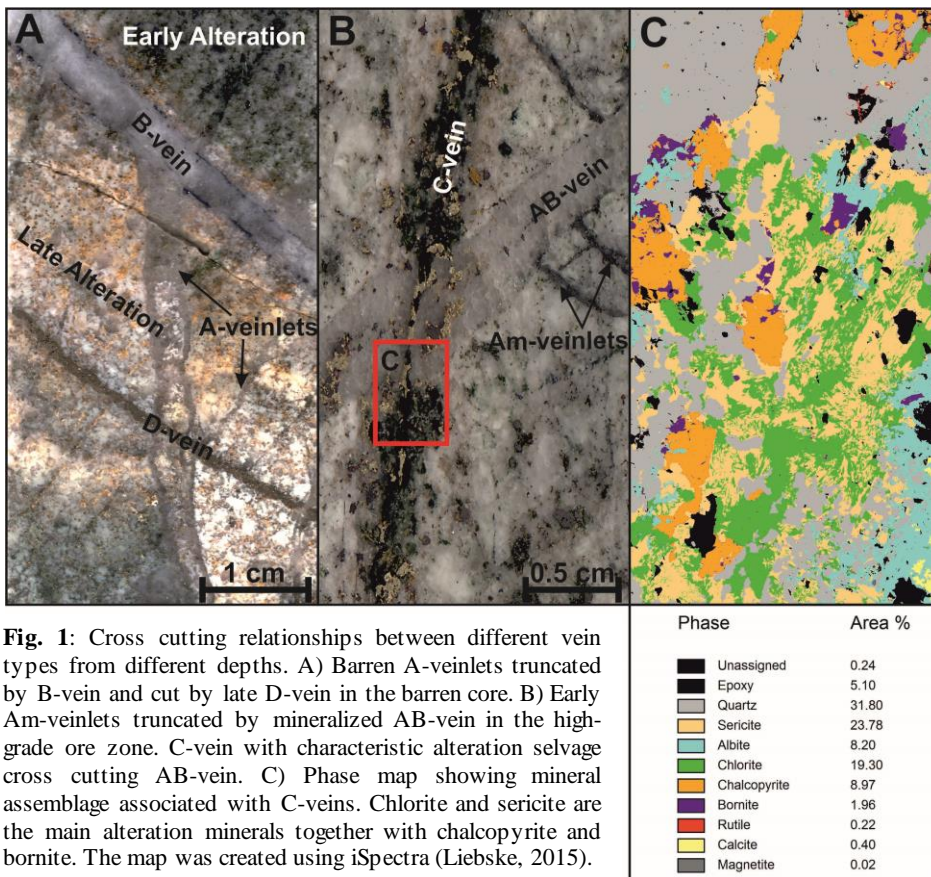


**Fig. 1:** Cross cutting relationships between different vein types from different depths. A) Barren A-veinlets truncated by B-vein and cut by late D-vein in the barren core. B) Early Am-veinlets truncated by mineralized AB-vein in the high-grade ore zone. C-vein with characteristic alteration selvage cross cutting AB-vein. C) Phase map showing mineral assemblage associated with C-veins. Chlorite and sericite are the main alteration minerals together with chalcopyrite and bornite. The map was created using iSpectra (Liebske, 2015).

earlier mineral assemblages to chlorite and sericite (Fig. 1B and C). Sulfides described as disseminated grains hosted by the porphyry rocks often appear to be aligned along such thin cracks that are barely visible. Earlier quartz veins seem to contain higher quantities of ore minerals close to intersections with C-veins. Furthermore, sulfide centerlines of B-veins show explicit similarities with C-veins.

*D-veins* represent the latest vein generation at Batu Hijau and consist entirely of pyrite with minor quartz grains (Fig. 1A). Feldspar-destructive alteration is associated with this late veining event, which seems to postdate the main mineralization stage.

### Hydrothermal Vein Quartz Textures and Sulfide Precipitation

CL-imaging of hydrothermal vein quartz revealed the occurrence of temporally superimposed quartz generations, representing a complex fluid history involving precipitation, dissolution, and recrystallization. In mineralized AB- and B-veins, at least three generations of quartz formation can be distinguished (Fig. 2). The first generation ( $Q_1$ ) is characterized by white to slightly grey shades and represents the largest portion of all quartz present. Locally, euhedral growth zones document crystal growth into open space. Dissolution fronts in  $Q_1$  followed by reprecipitation of medium grey quartz define the onset of  $Q_2$ . Both generations are closely related to each other and summarized as  $Q_{1-2}$ . Interestingly, sulfide grains are never completely enclosed in grains of the first two generations. In contrast, the last generation, marked by dark luminescent quartz filling cracks and

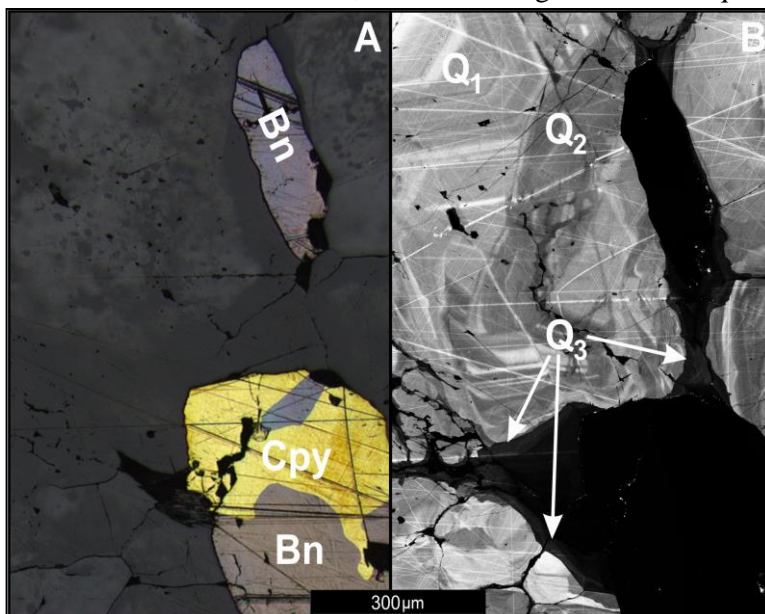


**Fig. 2:** Bornite (Bn) and chalcopyrite (Cpy) along the centerline of a B-vein from the high-grade ore zone. A) Reflected light image B) CL-image showing the different quartz generations.

*B-veins* are the latest quartz-dominated vein-type and characterized by their straight and planar wall rock contacts and prismatic quartz textures. The defining feature of B-veins is the presence of a centerline with euhedral quartz and a final fill of chalcopyrite and minor bornite, as well as traces of chlorite. In the lower parts of Batu Hijau, B-veins additionally contain anhydrite and minor molybdenite (Fig. 1A).

*C-veins* are fundamentally different compared to the previously described vein-types. They can be described as thin cracks partially filled by sulfide minerals and associated with mm-thin alteration halos marked by complete transformation of

interstitial spaces, seems to be genetically related to sulfide precipitation. All sulfide grains observed so far are embedded within this late quartz generation. Apparently, the late quartz generation follows the cross cutting C-veins, indicating their importance for ore formation. Irregular edges of  $Q_3$  and truncation of earlier growth zones are signs of dissolution processes (Frelinger et al., 2015) associated with the emergence of C-veins in Batu Hijau.

### Fluid Inclusion Petrography and Microthermometry

In the stockwork vein-system of Batu Hijau FIs are abundant and range in size from less than 5 to 50  $\mu\text{m}$  in diameter. Four different types of FIs can be distinguished based on phase proportions at room temperature: intermediate density (ID), aqueous (A), vapor-rich (V), and brine (B) inclusions. ID inclusions consist of two phases, vapor and liquid, in approximately equal proportions (Fig. 3A). In a few cases an opaque solid phase might be present. They are dominant in the deeper quartz veins but quantitatively decrease towards the mineralized part. The high-grade ore zone is marked by the predominance of V and B inclusions. B inclusions are characterized by one or multiple daughter minerals and a low vapor to liquid ratio (10-20 Vol.% vapor, Fig. 3B). In contrast, V inclusions show high vapor to liquid ratios, more than 70 Vol.% vapor, and no solid phase is present (Fig. 3C). Both inclusion types occur together in the same quartz grains belonging to  $Q_{1-2}$ . Trails of coexisting B and V inclusions (boiling trails) are no rarity. ID, V, and B inclusions always show negative crystal or rounded shapes. Aqueous (type A) inclusions are irregular, flat, and in some cases elongated. Like ID and V inclusions, they consist of two phases but with a low vapor to liquid ratio of less than 20 Vol.% vapor (Fig. 3D). In general, A inclusions are rather uncommon, occurring in most cases along the intersections of C-veins with earlier quartz veins. The  $Q_3$  generations contains predominantly tiny ( $< 1 \mu\text{m}$ ) A inclusions.

In order to get meaningful results, fluid inclusion assemblages (FIAs, as defined by Goldstein & Reynolds, 1994) were identified and used for microthermometry. Homogenization temperatures ( $T_H$ ) and salinities (in wt.%  $\text{NaCl}_{\text{eq}}$ ) of FIAs correlate with depth, vein type, and ore grades. ID inclusions homogenize to the liquid phase at around  $370^\circ\text{C}$  with salinities between 3 to 7 wt.%  $\text{NaCl}_{\text{eq}}$ . The homogenization temperatures and salinities of B inclusions increases from depth ( $320^\circ\text{C}$ , 35 wt.%  $\text{NaCl}_{\text{eq}}$ ) towards the high-grade zone ( $380^\circ\text{C}$ , 45 wt.%  $\text{NaCl}_{\text{eq}}$ ). Due to the high portion of vapor,  $T_h$  and salinities of V inclusions could not be precisely measured. However, rather high  $T_H$  of more than  $500^\circ\text{C}$  and low salinities in the range of 1 to 5 wt.%  $\text{NaCl}_{\text{eq}}$  can be presumed. A inclusions along C-veins show low  $T_H$  and salinities of around  $250^\circ\text{C}$  and 1 to 3 wt.%  $\text{NaCl}_{\text{eq}}$ .

### Implications for metallogenesis at Batu Hijau

The evolution of the hydrothermal fluid in time and space led to the formation of different vein-types associated with distinct alteration stages and eventually sulfide precipitation under favorable conditions. The early fluid history is preserved in quartz veins at greater depths in form of ID FIAs showing initial minimum entrapment temperatures of around  $370^\circ\text{C}$ . However, depending on pressure conditions, the original temperature of the fluid could be significantly higher, possibly in the range proposed by Garwin (2000). Separation into a low-density low-salinity vapor and a high-density high-salinity brine phase resulted from ascent to shallower depths and an associated drop in pressure. Although these fluid types are dominant in the high-grade ore zone, the two-phase fluid was probably preceding ore formation as revealed by CL-imaging. Sulfides precipitated either together with or shortly after the formation of  $Q_3$ . The presence of A FIs in

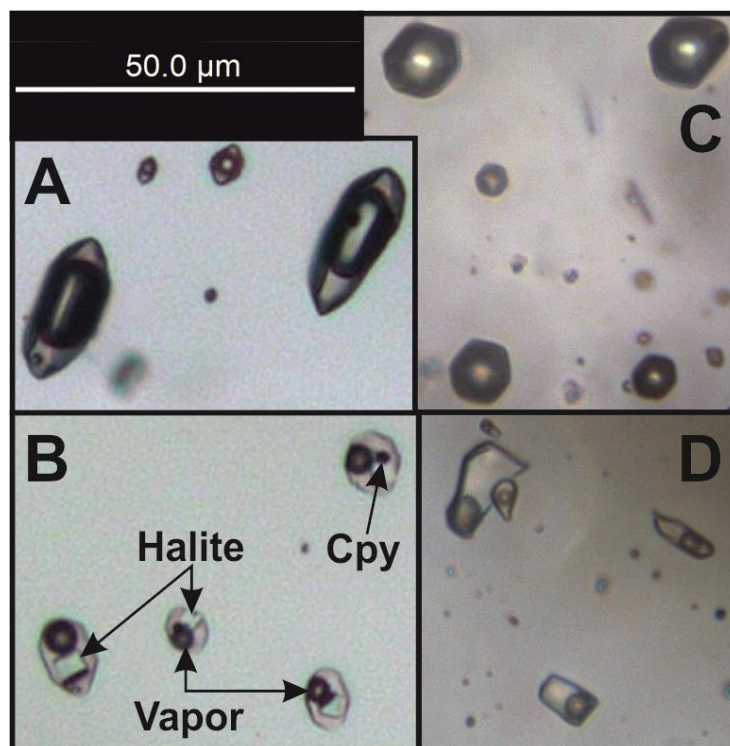


**Fig. 3:** FI-types occurring in hydrothermal quartz veins at Batu Hijau. A) ID inclusions from the barren core. B) B containing halite and chalcopyrite (cpy) daughter crystals and C) V inclusions from the high-grade ore zone. D) A inclusions close to C-vein.

combination with the general absence of V and B inclusions in Q<sub>3</sub> indicates that ore formation took place during a period of cooling from around 400°C to 250°C, whereby overlapping salinities permit the possibility of direct cooling of the magmatic vapour or a single-phase intermediate-density fluid to a denser aqueous fluid. Alternatively, a contribution of brine dilution by meteoric fluids may be a localising factor for the high-grade ore shell (Fekete et al., 2016). In summary, Batu Hijau is another porphyry copper ± gold deposit besides Butte (Rusk), Bingham Canyon (Landtwing et al., 2005), Elatsite, (Stefanova et al., 2014) and probably also Far South East (Hedenquist et al., 1998), where ore metal precipitation dominantly postdates the formation of the quartz stockwork veins and is more closely associated with quartz re-dissolution and incipient feldspar-destructive alteration.

### References:

- Arif J. & Baker T. (2004) Gold paragenesis and chemistry at Batu Hijau, Indonesia: implications for gold-rich porphyry copper deposits. *Miner. Deposita* 39:523-535.
- Clode C. Proffett J.M., Mitchell P., Munajat I. (1999) Relationships of intrusion, wall-rock alteration and mineralisation in the Batu Hijau copper-gold porphyry deposit. PACRIM'99 Proceedings: Bali Indonesia, pp 10-13.
- Fekete S., Weis P., Driesner T., Bouvier A.-S., Baumgartner L., Heinrich C.A. (2016) Contrasting hydrological processes of meteoric water incursion during magmatic-hydrothermal ore deposition: An oxygen isotope study by ion microprobe. *Earth Planet Sc. Lett.* 451:263-271.
- Frelinger S.N., Ledvina M.D., Kyle J.R., Zhao D. (2015) Scanning electron microscopy cathodoluminescence of quartz: Principles, techniques and applications in ore geology. *Ore Geol. Rev.* 65:840-852.
- Hedenquist J.W., Arribas A., Reynolds J.T. (1998) Evolution of an intrusion-centered hydrothermal system: Far Southeast-Lepanto porphyry and epithermal Cu-Au deposits, Philippines, *Econ. Geol.* 93:373-404.
- Imai A. & Ohno S. (2005) Primary ore mineral assemblage and fluid inclusion study of the Batu Hijau porphyry Cu-Au deposit, Sumbawa, Indonesia. *Resour. Geol.* 55.3:239-248.
- Imai A. & Nagai Y. (2009) Fluid inclusion study and opaque mineral assemblage at the deep and shallow part of the Batu Hijau porphyry copper-gold deposit, Sumbawa, Indonesia. *Resour. Geol.* 59:231-243.
- Garwin, S. L. (2000) The setting, geometry and timing of intrusion-related hydrothermal systems in the vicinity of the Batu Hijau porphyry copper-gold deposit, Sumbawa, Indonesia. Dissertation, University of Western Australia.
- Goldstein R.H. & Reynolds T.J. (1994) Systematics of fluid inclusions in diagenetic minerals. *Society for sedimentary geology short course* 31:199.
- Gustafson L.B. & Hunt J.P. (1975) The porphyry copper deposit at El Salvador, Chile. *Econ. Geol.* 70:857-912.
- Landtwing M.R., Pettke T., Halter W.E., Heinrich C.A., Redmond P.B., Einaudi M.T., Kunze K. (2005) Copper deposition during quartz dissolution by cooling magmatic-hydrothermal fluids: The Bingham porphyry. *Earth Planet Sc. Lett.* 235:229-243.
- Liebske C. (2015) iSpectra: An open source toolbox for the analysis of spectral images recorded on scanning electron microscopes. *Microsc. Microanal.* 21:1006-1016.
- Mitchell P.A., Proffett J.M., Dilles J.H. Geological review of the Batu Hijau porphyry copper-gold deposit, Sumbawa Island, Indonesia.
- Meldrum S.J., Aquino R.S., Gonzales R.I., Burke R.J., Suyadi A., Irianto B., Clarke D.S. (1994) The Batu Hijau porphyry copper-gold deposit, Sumbawa Island, Indonesia. *J. Geochem. Explor.* 50:203-220.
- Redmond P.B., Einaudi M.T., Inan E.E., Landtwing M.R., Heinrich C.A. (2004) Copper deposition by fluid cooling in intrusion-centered systems: New insights from the Bingham porphyry ore deposit, Utah. *Geology* 32:217-220.
- Rottier B., Kouzmanov K., Bouvier A., Baumgartner L.P., Wälle M., Rezeau H., Bendezi R., Fontboté L. (2016) Heterogeneous melt and hypersaline liquid inclusions in shallow porphyry type mineralization as markers of the magmatic-hydrothermal transition (Cerro de Pasco district, Peru). *Chem. Geol.* 447:93-116.
- Rusk B.G. & Reed M. (2002) Scanning electron microscope-cathodoluminescence analysis of quartz reveals complex growth histories in veins from the Butte porphyry copper deposit, Montana. *Geology* 30:727-730.
- Rusk B.G., Reed M.H., Dilles J.H., Kent A.J. (2006) Intensity of quartz cathodoluminescence and trace-element content in quartz from the porphyry copper deposit at Butte, Montana. *American Mineralogist* 91:1300-1312.
- Stefanova E., Driesner T., Zajacz Z., Heinrich C.A., Petrov P., Vasilev Z. (2014) Melt and fluid inclusions in hydrothermal veins: the magmatic to hydrothermal evolution of the Elatsite porphyry Cu-Au deposit, Bulgaria. *Econ. Geol.* 109:1359-1381.
- Zwyer (2010) Temporal and spatial evolution of hydrothermal, ore-related fluids in the Batu Hijau porphyry copper-gold deposit, Sumbawa (Indonesia). Unpublished Master Thesis, ETH Zürich.